



UNIVERSITY OF LEEDS

This is a repository copy of *Eco-reliable path finding in time-variant and stochastic networks*.

White Rose Research Online URL for this paper:
<http://eprints.whiterose.ac.uk/110452/>

Version: Accepted Version

Article:

Li, W, Yang, L, Wang, L et al. (3 more authors) (2017) Eco-reliable path finding in time-variant and stochastic networks. *Energy*, 121. pp. 372-387. ISSN 0360-5442

<https://doi.org/10.1016/j.energy.2017.01.008>

© 2017 Elsevier Ltd. Licensed under the Creative Commons Attribution-NonCommercial-NoDerivatives 4.0 International
<http://creativecommons.org/licenses/by-nc-nd/4.0/>

Reuse

Unless indicated otherwise, fulltext items are protected by copyright with all rights reserved. The copyright exception in section 29 of the Copyright, Designs and Patents Act 1988 allows the making of a single copy solely for the purpose of non-commercial research or private study within the limits of fair dealing. The publisher or other rights-holder may allow further reproduction and re-use of this version - refer to the White Rose Research Online record for this item. Where records identify the publisher as the copyright holder, users can verify any specific terms of use on the publisher's website.

Takedown

If you consider content in White Rose Research Online to be in breach of UK law, please notify us by emailing eprints@whiterose.ac.uk including the URL of the record and the reason for the withdrawal request.



eprints@whiterose.ac.uk
<https://eprints.whiterose.ac.uk/>

Accepted Manuscript

Eco-reliable path finding in time-variant and stochastic networks

Wenjie Li, Lixing Yang, Li Wang, Xuesong Zhou, Ronghui Liu, Ziyou Gao

PII: S0360-5442(17)30008-7

DOI: [10.1016/j.energy.2017.01.008](https://doi.org/10.1016/j.energy.2017.01.008)

Reference: EGY 10143

To appear in: *Energy*

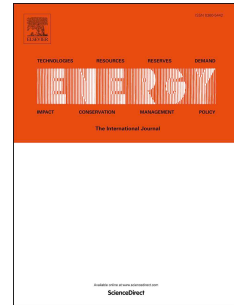
Received Date: 22 April 2016

Revised Date: 30 December 2016

Accepted Date: 3 January 2017

Please cite this article as: Li W, Yang L, Wang L, Zhou X, Liu R, Gao Z, Eco-reliable path finding in time-variant and stochastic networks, *Energy* (2017), doi: 10.1016/j.energy.2017.01.008.

This is a PDF file of an unedited manuscript that has been accepted for publication. As a service to our customers we are providing this early version of the manuscript. The manuscript will undergo copyediting, typesetting, and review of the resulting proof before it is published in its final form. Please note that during the production process errors may be discovered which could affect the content, and all legal disclaimers that apply to the journal pertain.



Eco-reliable Path Finding in Time-variant and Stochastic Networks

Wenjie Li^a, Lixing Yang^{a*}, Li Wang^a, Xuesong Zhou^b, Ronghui Liu^c, Ziyou Gao^a

^a State Key Laboratory of Rail Traffic Control and Safety, Beijing Jiaotong University, Beijing, 100044, China

^b School of Sustainable Engineering and the Built Environment, Arizona State University, Tempe, AZ 85287, USA

^c Institute for Transport Studies, University of Leeds, Leeds, LS2 9JT, United Kingdom

Abstract

This paper addresses a route guidance problem for finding the most eco-reliable path in time-variant and stochastic networks such that travelers can arrive at the destination with the maximum on-time probability while meeting vehicle emission standards imposed by government regulators. To characterize the dynamics and randomness of transportation networks, the link travel times and emissions are assumed to be time-variant random variables correlated over the entire network. A 0-1 integer mathematical programming model is formulated to minimize the probability of late arrival by simultaneously considering the least expected emission constraint. Using the Lagrangian relaxation approach, the primal model is relaxed into a dualized model which is further decomposed into two simple sub-problems. A sub-gradient method is developed to reduce gaps between upper and lower bounds. Three sets of numerical experiments are tested to demonstrate the efficiency and performance of our proposed model and algorithm.

Keywords: Eco-reliable Path Finding; Vehicle Emission; Time-variant and Stochastic Network; Lagrangian Relaxation Approach

1 Introduction

1.1 Motivation

Nowadays, the negative impact of automobiles on energy consumption, land use, noise and greenhouse gas (GHG) emissions, is still a significant topic in the transportation fields (see Knörr [18]). Among various pollutant emissions, GHG emissions and carbon dioxide (CO₂) are of particular concerns to the environment and the people's health. The international council on clean transportation pointed out that the transport sector is responsible for about one-quarter of energy-related GHG emissions worldwide, among which passenger vehicles account for nearly half of this total emissions, and are predicated to remain the predominant source of these emissions for the foreseeable future. According to technical summary in climate change 2014 (Edenhofer et al. [7]), the global transport sector accounts for 27% of total energy consumption and 6.7 GtCO₂ direct emissions in 2010. The baseline CO₂ emissions in transport sector is projected to increase to 9.3-12 GtCO₂/year in 2050. Due to the large size of global vehicle fleet and its high rate of growth, CO₂ emissions produced by passenger vehicles will remain one of the greatest challenges for the governments.

*E-mail address: lxyang@bjtu.edu.cn (L. Yang)

To reduce CO₂ emissions in the transport field, public authorities have mandated a variety of effective policies in different areas nowadays. For instance, in Beijing city, the government has adopted the odd-and-even license plate driving rule to further reduce individual trips and their emissions efficiently because of the serious haze. Also, in the United States, the Department of Energy's Advanced Research Projects Agency-Energy (ARPA-E) (see <https://arpa-e.energy.gov/?q=arpa-e-programs/nextcar>) program has supported a number of high-profile projects for its Next-Generation Energy Technologies for Connected and Autonomous On-Road Vehicles (NEXTCAR), in which intelligent eco-routing is a key component to use extensive data analytics to assign routes for minimizing energy consumption. Meanwhile, in the European Union, under the Framework Programme 7 (see <http://www.reduction-project.eu/>), a number of collaborative research projects, such as REDUCTION, were designed for reducing environmental footprint based on eco-routing and driver behavior adaptation. Additionally, in real life, travelers are more likely to rely on navigation systems to capture real-time road conditions and find their appropriate paths with route guidance. Thus, on the level of management, if the government would like to impose constraints on eco-routing, it is typically convenient and practical for public authorities to manage individual trips. With the aforementioned various backgrounds with respect to eco-routing applications, this study intends to offer ecological and effective route guidance strategies to policy makers with eco-reliable path choice methods.

1.2 Literature Review

A variety of theoretical researches about CO₂ reductions have been conducted, and mandatory policies have been implemented up to now. For example, Xu and Lin [36] used vector autoregressive model to analyze the influencing factors for CO₂ emissions in Chinese transport sector, and concluded that energy efficiency plays a dominant role in reducing CO₂ emissions. Walmsley et al. [34] applied the modified carbon emissions pinch analysis method to investigating the feasibility of several proposed regulatory solutions on emission reductions of the New Zealand government. Since the European emission trading system (EU ETS) covers an increasing amount of overall European CO₂ emissions except the transport sector's, Heinrichs et al. [15] utilised a model-based approach including an electricity system model (i.e., package for emission reduction strategies in energy use and supply in Europe) and a road transport model (i.e., CO₂ emission mitigation in the transport sector) to enlarge the EU ETS, which can reduce the overall CO₂ emissions and make mitigation efforts in road transport field. From the mid-twentieth century, the government regulations, such as tailpipe emission standards and breakthrough technologies (e.g., the three-way catalytic converter), have made significant achievements in the reductions in passenger vehicle emissions. Hao et al. [16] analysed the impacts of the recent pollution mitigation policies in China and concluded that fuel consumption regulations played an essential role in effectively offsetting the impacts of vehicle pollution. The first emission standards for passenger vehicles was established by California in the 1960s, which was soon followed by the rest of the United States, Japan and Europe. According to Hu et al. (see [14]), imposition of strict emission standards is adopted by the governments to reduce emissions. For example, the regulations on CO₂ emissions set up by the environmental protection agency (EPA) of the United States require all new passenger vehicles' CO₂ emissions to be reduced from 268 gram per mile (gpm) in 2012 to 225 gpm in 2016. In Europe, the CO₂ emission standards are even more aggressive, requiring all light-duty vehicles introduced after 2012 to emit 120 gram per kilometer or less. However, from travelers' point of view, these emission standards only regulate the average CO₂ emissions of per unit driving distance for new vehicles, which are not specifically related to individual trips.

Practically, the CO₂ emissions have close relationships to different factors. For instance, Palmer [29]

carried out an in-depth study by integrating routing and emissions model for freight vehicles and demonstrated the significant role of vehicle speed in CO₂ reductions. Rilett and Benedek [30] showed that vehicle emissions do not change monotonically with travel speed, and the conflict between these two aspects may exist. Usually, the lowest CO₂ emissions rate is found to be at speed around 55 – 60 miles per hour (see, e.g. <http://www.mpgforspeed.com>), while travel times in some circumstances are not minimal at these speeds. Thus, a trade-off should be made between these two factors in order to find a green and efficient path for travelers. Studies by Tzeng and Chen [33], Aziz and Ukkusuri [2] and Yin and Lawphongpanich [42] showed that a compromise can be made between travel time and emission in formulating a multi-objective optimization model. In Bektas and Laporte [5] and Li et al. [19], the travel times and emissions were translated into monetary cost. However, the resulted optimal paths are very sensitive to the cost parameters used. Additionally, the CO₂ emission is also closely related to the fuel consumption. For instance, Akcelik et al. [1], Simpson [31] and Barth et al. [4] proposed different methods, i.e., the aaSIDRA (signalised intersection design and research aid) and aaMOTION, the parametric analytical model of vehicle energy consumption and the comprehensive modal emission model, respectively, to identify the relationship between fuel consumption and emission rates. Li et al. [20] formulated a model of CO₂ emission to test the most cost-effective fuel option.

From the above analyses, it is clear that the CO₂ emission is not only related to management policies, but also related to activities of vehicles on the microcosmic level (above all the route choice of different vehicles). In individual trips, a variety of pre-trip guidance systems (e.g., navigation system) are often used to identify the real-time road conditions, and then to generate a set of available path information. To reduce the CO₂ emissions in the vehicle trip, many researchers developed different approaches to find the green paths. For instance, Bektas and Laporte [5] extended the traditional vehicle routing problem with an objective to reduce CO₂ emissions and developed a pollution routing problem. Erdogan and Miller-Hooks [6] considered a fleet of vehicles and the limited refueling infrastructure, and formulated a green vehicle routing problem to reduce fossil-fuel usage. Ehmke et al. [9] minimized the time-dependent emissions in vehicle routing problems in urban areas. Zhou et al. [44] integrated a simplified emission estimation model and mesoscopic dynamic traffic simulator to efficiently evaluate emission impacts of traffic management strategies. Zeng et al. [45] predicted the vehicle CO₂ emissions and determined an eco-friendly path which satisfies the minimum CO₂ emissions and travel time budget simultaneously. Typically, if the emission constraints can be imposed on the path finding process in the navigation systems, the CO₂ emission about passenger vehicles can be effectively reduced through providing drivers with low-carbon route guidance. To our knowledge, the existing researches do not specifically consider both the dynamics and randomness of the travel time and emissions in the path finding problems. In the literature, for the path-finding process in time-variant and stochastic networks, many optimal strategies related to travel time have been proposed with various evaluation indices, such as the least expected travel time (Miller-Hooks [24]; Wang et al. [35]; Yang and Zhou [38], Yang et al. [41]), the probability of on-time arrival (Fan et al. [11]; Nie and Wu [27]; Samaranyake et al. [32]), the minimum possible travel time (Nielsen [26]), etc. Among them, the least expected travel time method has been widely applied in route-finding studies. For example, Miller-Hooks [24] used a priori least-expected time path and a set of strategies to improve routing decisions. Yang and Zhou [38] adopted a Lagrangian relaxation-based solution algorithm to reformulate and solve the least expected time path model. Furthermore, Wang et al. [35] investigated a priori least expected time paths in fuzzy and time-variant transportation networks. Nielsen [26] considered route choice problems in stochastic and time-dependent networks, and employed the minimizing expected travel time and cost as the given criteria. As for the reliable path finding, Fan

et al. [11] proposed a new concept to maximize the probability of on-time arrival whose arrival time is on time or earlier, while Samaranyake et al. [32] presented a new optimality criterion to minimize the probability of arriving on time at a destination given a departure time and a time budget. Nie and Wu [27] considered on-time arrival probability with first-order stochastic dominance and a label-correcting algorithm. As for the low emission/energy efficiency based space-time paths for multiple trains, interested readers can refer to Huang et al. [17] and Yin et al. [42].

1.3 Contributions of This Study

With the above analyses, we can see that (1) very few studies take both random and dynamic characteristics into consideration during the green path finding process; (2) no research has been found to consider both the reliability and low-emission in evaluating the generated paths. With these concerns, this paper aims to find an eco-reliable path in time-variant and stochastic networks to offer a routing guidance for travelers within emission standards of government regulators. The proposed approaches can be expected to provide effective pathing finding strategies for reducing the CO₂ emissions on the vehicle-operation-based levels. Specifically, the main contributions of this study can be summarized as follows:

(1) To characterize the dynamics and randomness of the network, we consider two types of time-variant link weights, i.e., link travel times and link emissions. In detail, link emissions are closely related to average link speed where the quadratic functions of emission-speed relationship can be derived from MOVES (Motor vehicle emission simulator). A sample-based representation method is used to capture the randomness, in which each sample corresponds to time-variant link travel time and link emission data over the entire network through considering the correlation of randomness. This kind of representation typically can include the real-world detected data into the decision-making processes.

(2) We formulate an linear integer programming model to generate the eco-reliable paths, in which the objective function is the on-time arrival probability corresponding to different space-time paths. A physical path which has the largest chance of ecology and reliability is termed as the eco-reliable path. To show the emission limit, a threshold is particularly given to formulate the emission constraints. That is, it is required that the expected emission is less than vehicle emission standards (i.e., the given threshold) imposed by government regulators.

(3) Finally, the Lagrangian relaxation approach is introduced to relax the primal model into a relaxed model by dualizing hard constraints. The dualized model is further decomposed into two types of sub-problems (i.e., a standard shortest path problem and a simple univariant linear problem) and a constant, which can be solved by the label correcting algorithm, a simple single-value linear programming and the given Lagrangian multipliers, respectively. The sub-gradient method is developed to obtain the tight gap between lower and upper bounds. The optimal solutions provide an effective guidance for travelers with low-carbon emission concerns.

To explain the merits of our research clearly, we further make a comparative summary of our paper in Table 1 through comparing with several closely related references.

[place Table 1 about here]

The rest of this paper is organized as follows. Section 2 gives a detailed description of the eco-reliable path model in time-variant and stochastic networks. The definition of the most eco-reliable path and the 0-1 integer programming model are further proposed. In Section 3, we decompose the 0-1 integer programming model by the Lagrangian relaxation approach through introducing a series of

Lagrangian multipliers. Three sets of numerical experiments are implemented in Section 4 to demonstrate the efficiency and performance of our proposed model and algorithms. At last, a conclusion of this paper is made in Section 5.

2 Problem Statement

This section aims to give a detailed statement for the problem of interest, including the structure of involved space-time networks, input data representation, evaluation index, and mathematical formulation.

2.1 Structure of Time-variant and Stochastic Networks

The eco-reliable path finding problem is defined in a directed, well-connected transportation network $G = (M, N)$, in which M and N represent the sets of nodes and traffic links, respectively. To effectively reflect the dynamic characteristics of transportation networks, the time horizon is first divided into a set of discrete timestamps, denoted by $T = \{t_0, t_0 + \delta, t_0 + 2\delta, \dots, t_0 + K\delta\}$, where δ is assumed to be the duration of the short time interval during which no perceptible changes of travel times happen in the considered transportation network, and K is a sufficiently large positive integer to ensure that the time period from t_0 to $t_0 + K\delta$ covers the entire operating time. In routing process, one is required to start from the origin at time t_0 and arrive at his/her destination at some timestamp in time interval $[t_0, t_0 + K\delta]$. A time threshold is also given to specify the on-time arrival timestamp in the network, denoted by \hat{T} . That is, the on-time arrival means that a traveler arrives at the destination before the time \hat{T} . In practice, this time threshold can be set by considering traveler's expected arrival time.

Besides dynamics, another key characteristic in the urban transportation network is the randomness. For instance, we assume that a traveler departs from his/her origin (e.g., home) to the office everyday. The practical travel times often fluctuate even with the same departure time due to the randomness of the link travel times. To simultaneously capture the dynamic and randomness of transportation networks, a physical network will be extended into a series of sample-based space-time networks, denoted by $G^s = (M^s, N^s)$, $s \in \{1, 2, \dots, S\}$, where s represents the index of different samples and S represents the total number of samples. Corresponding to M and N in physical network, M^s and N^s represent the sets of space-time nodes and space-time links, respectively. Furthermore, M^s can be described by $M^s = \{i_t | i \in M, t \in T\}$, in which $i_t \in M^s$ means the state of node i at time stamp t . Similarly, N^s can be described by $N^s = \{(i_t, j_{t'}) | (i, j) \in N, t + a_{ijt}^s = t', t_0 \leq t \leq t' \leq t_0 + K\delta\}$, where a_{ijt}^s is the link travel time along link (i, j) with the departure time t over sample s . As the focus of this research is to generate the reliable paths, a dummy destination node $J'_{t_0+K\delta}$ is added to each space-time network to show the end of space-time path searching process. Accordingly, the dummy destination node J' and dummy link (J, J') are also added to the physical network. In the literature, this type of space-time network representation method has been effectively applied to a variety of research fields, such as traffic network design (Liu and Zhou [21]), congested traffic flow assignment (Lu et al. [22]), the vehicle routing problem (Mahmoudi and Zhou [23]), train scheduling problems (Yang et al. [39, 40]), etc.

In this paper, we use the sample-based approach to capture complex temporal and spatial travel time corrections in a traffic network. Particularly, historical travel times over different days can be used to construct samples. The travel time corrections can be contributed by physical bottlenecks and a number of delay resources such as incidents, road construction, severe weather conditions and special events. If there are more vehicles and possible delays, the historical link travel times can be more complex.

An illustrative space-time network over one sample is shown in Fig.1, in which the x -axis displays a planning time horizon and $t_n = t_0 + n\delta$, $n \in \{0, 1, 2, \dots, 5\}$. If we consider a total of S samples to capture randomness in the modeling process, the physical network needs to be extended into S sample-based space-time networks, and each space-time network has its own time-variant link travel times and travel emissions. Particularly, if we suppose each sample of the space-time path has the same occurrence probability, the probability of each space-time path is $1/S$.

[place Fig. 1 about here]

In this figure, we consider a physical path from node I to node J . When we embed the time horizon into this physical path, we can easily deduce a two-dimensional network associated with both spatial and temporal characteristics. In this space-time network, each arc is related to both physical link and its travel time (i.e., the entering and departure times along this link). As shown, timestamp \hat{T} (i.e., t_3) is the predetermined time threshold to indicate the desirable paths. We take two space-time paths as an illustration to show on-time arrival features. In detail, one path (marked by green color) departs from the origin at t_0 and arrives at the destination at t_2 , while the other one (marked by blue color) departs from the origin at t_1 and arrives at the destination at t_4 (i.e., one time interval dwelling at initial node). Typically, if a path arrives at any space-time node of the destination before \hat{T} , this path should be a on-time arrival path. With this concern, the space-time path with green color is a desirable path in the process of decision-making. On the contrary, the blue space-time path should be undesirable due to its late arriving time.

In this research, all the formulations of the eco-reliable path finding process are proposed on the basis of the framework of the space-time network mentioned above. In practice, each link is actually related to both travel time and emission. Then the space-time network with this two attributes will be discussed in the following sections to generate the eco-reliable pathing guidance for the travelers. For the completeness of this study, we first list all the symbols and parameters that can be used in the formulating process, shown in Table 2.

[place Table 2 about here]

2.2 The most eco-reliable path

In this section, we intend to clearly state the problem of interest in our study. In the path finding process, it is widely recognized that the traveler needs to consider two indexes to indicate the priorities of the selected paths, i.e., path travel time and path emission. According to Rilett and Benedek [30] and Nagurney [25], there possibly exists a confliction between the actual travel time and emissions because the emission does not change monotonically with respect to average travel speed. Then, with the time-variant and random characteristics in the physical network, how to find a desirable path turns out to be a significant issue for the travelers.

Next, we propose the concept of eco-reliable path to well address the green path finding with the restricted emission. In this definition, we first give an expected threshold by emission standards to indicate the ecological path choice so as to reduce the CO₂ emissions in the trip. The reliability refers to the probability of on-time arrival at the destination with different random samples through pre-specifying an on-time arrival threshold. Then in the formulation, the aim is to find a physical path with the maximized on-time arrival probability under the constraints of emission restrictions. To clearly address this issue, the following discussion gives an illustration to show how to produce the desirable eco-reliable paths in the physical network.

[place Fig. 2 about here]

In this illustration, we also consider a physical path with three nodes. To characterize the randomness with respect to the link travel time, we here take four samples into the consideration with equal probability (i.e., 0.25), where each sample corresponds to a set of time-dependent link travel times. Meanwhile, we consider link emission constraint in this illustration. Because a vehicle's emissions on one link are influenced greatly by its travel time on this link, there is necessarily a corresponding amount of emissions for each time-dependent link travel time. Accordingly, there is a quadratic function with respect to the emission rate (gram/mile) and the average speed (Li et al. [19]). In this sense, link emissions also have time-variant and stochastic characteristics deduced by the sample-based time-dependent link travel times, and could be pre-given over each sample-based space-time arc in our study.

To evaluate this physical path, we first generate the least time space-time paths in different sample-based space-time networks (marked by different colors, and the numbers represent the link emissions), in which the desirable departure time is set as time 0, and a departure time window at original node can be set as $[0, 2]$. Then we employ these pathing information to determine the feasibility and priority of the considered physical path. Firstly, we calculate the expected emission on these adaptively generated space-time paths. If this expected emission satisfies the requirements, then the physical path can be regarded as a feasible solution to the original problem. However, if the expected emission threshold is set as a relative small value, this physical path possibly violates this constraint, leading to its infeasibility. For a given physical path, the objective can be defined as the on-time arrival probability over these space-time paths, where the corresponding numerical characteristics are given in the following table.

[place Table 3 about here]

In Table 3, we calculate all the numerical characteristics of different space-time paths, including departure time, path travel time, path emissions, etc. The on-time arrival threshold is set as 5. Then, the corresponding on-time arrival probability and expected emission turn out to be 50% and 7 separately. If the expected emission satisfies the constraints, this physical path should be a feasible path with the objective 50%; otherwise it is an infeasible path. Once a feasible physical path with the maximum probability of arriving on time (AOT) is obtained, it is the optimal solution to the problem of interest.

2.2.1 The ecology of the most eco-reliable path

Usually, there are various emissions for gasoline-fueled passenger cars. For clarity, we give a common ingredients of emissions, listed below (see <https://www3.epa.gov/otaq/consumer/420f08024.pdf>).

[place Table 4 about here]

These pollutants all have hazardous impacts on the environment. We can observe from Table 4 that the CO₂ emission with the largest volume is the predominant emission obviously. Additionally, the CO₂ emission is the most concerning issue as it has direct consequences on the human health (e.g., pollution) and indirect ones (e.g., climate change). The transportation sector accounts for about 31 percent of total U.S. CO₂ emissions and 25 percent of total U.S. GHG emissions in 2014 (see <https://www.epa.gov/ghgemissions/overview-greenhouse-gases>). Governments have mandated a lot of regulations to reduce CO₂ emissions, and the eco-reliable route choice problem considering CO₂ emissions can offer regulatory solutions to policymakers. Barth et al. [4] proposed approaches to estimate the emissions of an individual vehicle under real driving conditions. These models are required to input

detailed vehicle operating parameters, such as instantaneous speed, acceleration profile and engine power. In reality, emissions of passenger vehicles are determined by several factors, such as vehicle type, model years, average emission conditions (e.g., speed) and so on. An aggregated approach proposed by Yin and Lawphongpanich [42] estimated average emission rates from these aggregated parameters, and was widely used to estimate the impacts of emissions on route choice in various transport models for large metropolitan areas. In this paper, we take link speeds as the predominant factor in decision making, because they determine the time that a passenger vehicle traverses a link, and the rate of CO₂ emissions accordingly (see Li et al. [19]). Because it is difficult to estimate real-time emission conditions to make routing decisions in advance as they fluctuate significantly, the motor vehicle emission simulator (MOVES) based on the aggregated approach method is adopted in this paper to estimate passenger vehicle emissions. Especially, the relationship between CO₂ emission rates and average link speed can be built after analysing the outputs of MOVES.

MOVES estimates emissions using a model based approach which utilizes two factors to affect emissions, i.e., the emission source bin and the vehicle operating mode bin. The emission source bin classifies emissions by vehicle characteristics, such as fuel type, engine type, model years, loaded weight, and engine size. The operating mode bin referring to vehicle operating conditions classifies emissions by second-by-second vehicle activities, called vehicle specific power (VSP), which is a measure to evaluate the power demand of a vehicle under various modes and instantaneous speed changes, and differentiated by average speed, road type and vehicle type. According to EPA [8], MOVES assigns two emission rates for the combined emission source bin and the operating mode bin separately. Next, an overall emission rate is produced by aggregated emission rates for each source-operating type. Once a matrix of emission rates is generated for each source-operating type, we can also obtain a few correction factors corresponding to emission rates to adjust the influence of temperature, air conditioning, and fuel effects. After analyzing a matrix of emission rates by vehicle speed corresponding to each road type, vehicle type and analysis year, the emission-speed relationship will be obtained in form of a quadratic function.

In the following, we give a detailed procedure of the working procedure, which is also displayed by a flow chart in Fig. 3.

Step 1: Input a series of key parameters (e.g., vehicle type, fuel type, analysis year, etc.) about a specific area into MOVES;

Step 2: Classify all the input activities into different bins, i.e., the emission source bin and the vehicle operating mode bin;

Step 3: Produce an overall emission rate for each source-operating type;

Step 4: Obtain emission-speed relationship in form of a quadratic function by analysing a matrix of emission rates and average vehicle speed.

[place Fig. 3 about here]

Next, we need specify the link distance l_{ij} to calculate the detailed link average speed v_{ij} and link emissions e_{ij} with the given link travel time a_{ij} . Evidently, parameters a_{ij} and v_{ij} are in inverse proportion, and a linear relationship approximately holds between e_{ij} and its unit distance emission rate $y_e(v_{ij})$ which is a quadratic function and can be calculated from above procedures. Typically, for each given link travel time, we can also deduce its link emission through Eq. (1).

$$v_{ij} = l_{ij} \div a_{ij}, e_{ij} = l_{ij} \times y_e(v_{ij}) \quad (1)$$

In this study, we adopt the sample-based time-dependent link travel times to capture the dynamics and

randomness of the considered network. Thus, with the given emission rate function $y_e(v)$, the time-variant and stochastic link emissions can also be easily calculated corresponding to the given link travel times.

Since this research aims to jointly consider both travel efficiency and ecology, in the following we particularly handle the emission as a system constraint condition through embedding the expected value operator. In detail, for the sample-based space-time paths along any given physical path, we first calculate the expected emission on these space-time paths. Then, it is required that the expected path emission should not exceed a predetermined emission threshold. In the sample-based space-time network, x_{ijt}^s is a binary variable indicating whether a time-dependent arc is selected or not. We define E_{total} (unit: kilograms CO₂) as the expected emissions, calculated below, in which the probability of each sample is supposed to be $1/S$.

$$E_{total} = \frac{1}{S} \sum_{s=1}^S \sum_{(i,j) \in N} \sum_{t \in T} e_{ijt}^s x_{ijt}^s \quad (2)$$

Then, the expected emission constraint can be formulated as follows:

$$E_{total} \leq \bar{E}, \quad (3)$$

where \bar{E} is an emission threshold to denote the limit for total emissions of a physical path. Actually, to offer a route guidance under the government policy, different countries have published their own vehicle emission standards for various types of vehicles, e.g., passengers cars, light-duty trucks, heavy-duty vehicles, heavy-duty engines and motorcycles. Total standard CO₂ emissions of one travel activity can be calculated by travel distance and emission with unit of kilograms CO₂/mile. For notation simplicity, Eq. (3) can be simplified as Eq. (4) since S is a constant.

$$\sum_{s=1}^S \sum_{(i,j) \in N} \sum_{t \in T} e_{ijt}^s x_{ijt}^s \leq S \cdot \bar{E} \quad (4)$$

2.2.2 The reliability of the most eco-reliable path

This paper aims to provide a path that has the maximum probability of on-time arrival for route guidance. To evaluate a physical path, we need to first generate the sample-based shortest paths over different space-time networks. These information can be used to calculate the reliability of this physical path according to Yang and Zhou [43]. To show this idea clearly, Fig. 4 is given as an illustration of four shortest space-time paths which arrive at destination at t_2 , t_4 , t_6 and t_7 , respectively. If the on-time arrival threshold \hat{T} is assumed to be t_5 , the former two space-time paths are typically desirable, while the other ones are undesirable paths.

To describe the reliability of eco-reliable paths, we denote X^s and $T(X^s)$ as the sample-based space-time path and its arrival time on sample s . The desirable space-time paths are obtained by comparing their arrival time with the on-time arrival threshold \hat{T} , and Ψ is defined as the set of desirable space-time paths corresponding to one physical path, where $|\Psi|$ is the number of these paths. In detail, Eq. (5) defined below enumerates all the desirable space-time paths.

$$\Psi = \{X^s, s \in \{1, 2, \dots, S\} \mid T(X^s) \leq \hat{T}\} \quad (5)$$

[place Fig. 4 about here]

Next, with the definition of Ψ , we can calculate the on-time arrival probability to show the reliability degree of the corresponding physical path. Since this paper assumes the equal probability for each sample

(i.e., $P_s = 1/S$), it is easy to calculate the on-time arrival probability by Eq. (6).

$$P(\Psi) = |\Psi|/S \quad (6)$$

For instance, we totally produce four least time space-time paths over different samples in Fig. 5. Since the on-time arrival threshold is $\hat{T} = 5$, we then deduce $\Psi = \{X^1, X^2\}$. Thus, the on-time arrival probability of this physical path is 0.5.

This paper aims to find the most eco-reliable path in the considered network, the focus is to maximize the on-time arrival probability over different physical paths with the given emission threshold. Equivalently, maximizing the on-time arrival probability corresponds to the minimization of the late arrival probability. Then with the set Ψ , we can compute the late arrival probability, which will be used as the objective function in the modelling process. Specifically, we first consider the complementary set Ψ^c of Ψ . Then, the late arrival probability can be calculated by Eq. (7).

$$P(\Psi^c) = 1 - P(\Psi) = 1 - |\Psi|/S = (S - |\Psi|)/S \quad (7)$$

Clearly, the key point in calculating the late arrival probability is to compare the arrival time of each sample-based path with the on-time arrival threshold. Note that all the generated space-time paths are required to terminate at the dummy space-time node. Then, the arrival time at physical destination of each path is actually the entering time of selected dummy link. In the modelling process, $x_{JJ't}^s$ is defined as a binary decision variable of link (J, J') on entering time t over sample s , in which J and J' are the physical and dummy destination nodes. Thus, to calculate the late arrival probability, it is necessary to consider the entering times of selected dummy space-time links after the time threshold \hat{T} (see Yang and Zhou [43]). With this consideration, the objective function is formulated as follows.

$$\min \Gamma_t = \frac{1}{S} \sum_{s=1}^S \sum_{t > \hat{T}} x_{JJ't}^s \quad (8)$$

For simplicity, we can further rewrite an equivalent formulation as follows since the input parameter S is a constant, i.e.,

$$\min \Gamma_t = \sum_{s=1}^S \sum_{t > \hat{T}} x_{JJ't}^s \quad (9)$$

2.3 Mathematical model of the most eco-reliable path finding

The focus of this study is to generate a physical path on the given OD (origin-destination) pair such that the reliability criterion is maximized. To simplify the notation, we only handle the path finding over different sample-based space-time networks instead of directly over the physical network. A project constraint from the space-time path to the unique physical path is particularly introduced to achieve our goal. Thus, some additional system constraints should also be taken into consideration to formally formulate the rigorous optimization model, including **the space-time flow balance constraint, the unique path constraint and the binary constraint**. In detail, to guarantee that all the selected space-time links can constitute a path from an origin (I, t_0) to destination $(J', t_0 + K\delta)$ in the space-time network, **the space-time flow balance constraint** that balances incoming and outgoing flows is formulated as follows.

$$\sum_{(i_t, j_t') \in N^s} x_{ij_t}^s - \sum_{(j_t', i_t) \in N^s} x_{j_t' i_t}^s = \begin{cases} 1, & i = I, t = t_0 \\ -1, & i = J', t = t_0 + K\delta, s \in \{1, 2, \dots, S\} \\ 0, & \text{otherwise} \end{cases} \quad (10)$$

In addition, in order to guarantee the uniqueness of the corresponding physical paths over different samples, we here project each selected space-time arc to its physical link by summing all the corresponding space-time arc selection indicators over the considered time horizon. Thus, we provide the following **unique path constraint** through considering the projected relationship.

$$\sum_{t \in T} x_{ijt}^s = \sum_{t \in T} x_{ijt}^{s'}, \forall (i, j) \in N, s, s' \in \{1, 2, \dots, S\} \quad (11)$$

To generate the optimal path in transportation networks through minimizing the late arrival probability over all samples, the integer programming model of the eco-reliable path finding problem can be formulated as below.

$$\left\{ \begin{array}{l} \min \Gamma_t = \sum_{s=1}^S \sum_{t > \hat{T}} x_{J'J''}^s \\ s.t. \\ \text{constraints (4), (10), (11)} \\ x_{ijt}^s \in \{0, 1\}, \forall (i, j) \in N, s \in \{1, 2, \dots, S\}, t \in T \end{array} \right. \quad (12)$$

In this model, the first constraint aims to control the total emission under the pre-specified emission standards; the second constraint generates different space-time paths over individual samples; the third constraint project the different space-time paths to a unique physical path. With the reliability representation in the objective, this model aims to generate the most eco-reliable path over the considered physical network.

3 Lagrangian relaxation-based solution approach

Since it is difficult to solve the model (12) due to several complex constraints, we need to design an efficient method to deal with these hard constraints. Note that this model can be regarded as a generalized shortest path problem with different side constraints which can be effectively solved by the Lagrangian relaxation approach (For more details of Lagrangian, interested readers can refer to Fisher [10, 12], Geoffrion [13], etc.). Thus, we aim to develop an efficient Lagrangian relaxation-based approach to relax some hard constraints of this model, through which the dualized model can be decomposed into a series of shortest path problems and simple sub-problems. The shortest path problems can be efficiently solved by the label correcting algorithm (see Bertsekas [3]). In the solution process, the sub-gradient method will be used to update the Lagrangian multipliers, and iteratively produce the tightest lower bound and the near-optimal solutions to the original problem. The detailed procedure are detailed as below.

3.1 Hard constraints relaxation

In this subsection, the efficient lower bound estimator should be developed by reformulating the model (12). The space-time flow balance constraint (10) in the model is tractable with the label correcting algorithm, and the other two constraints (4) and (11) are regarded as the hard constraints.

There are a total of $S(S - 1)/2$ equalities for each link in the hard constraint (11), and it is difficult to relax this constraint into the objective function. Actually, the constraint (11) essentially equals to the

following constraint.

$$\sum_{t \in T} x_{ijt}^1 = \sum_{t \in T} x_{ijt}^2, \sum_{t \in T} x_{ijt}^2 = \sum_{t \in T} x_{ijt}^3, \dots, \sum_{t \in T} x_{ijt}^{S-1} = \sum_{t \in T} x_{ijt}^S, \forall (i, j) \in N \quad (13)$$

Next, the constraint (13) can be further equivalently reformulated into the following constraint according to Yang and Zhou [38].

$$\sum_{t \in T} x_{ijt}^s - \bar{x}_{ij} = 0, \forall (i, j) \in N, s \in \{1, 2, \dots, S\} \quad (14)$$

$$\bar{x}_{ij} = \frac{1}{S} \times \sum_{s=1}^S \sum_{t \in T} x_{ijt}^s, \forall (i, j) \in N \quad (15)$$

In the dualized process of Lagrangian relaxation approach, a number $|N| * (S - 1)$ of Lagrangian multipliers for constraint (13) should be introduced, while a number $|N| * (S + 1)$ of Lagrangian multipliers for constraint (14) and (15) should be considered. In addition, we can also relax the constraint (14) as an inequality below according to Yang and Zhou [38].

$$\sum_{t \in T} x_{ijt}^s - \bar{x}_{ij} \leq 0, \forall (i, j) \in N, s \in \{1, 2, \dots, S\} \quad (16)$$

After reformulating the hard constraint (11) into constraints (15) and (16), these two side constraints together with constraint (4) need to be relaxed into the objective function by introducing three sets of multipliers, i.e., multipliers $\alpha \geq 0$ for constraint (4), multipliers $\beta_{ij}^s \geq 0$ for constraint (15) and multipliers $\gamma_{ij} \in R$ for constraint (16), where $(i, j) \in N, s \in \{1, 2, \dots, S\}$. To further explain the solution process straightforwardly, Table 5 lists all symbols related to the Lagrangian relaxation-based approach.

[place Table 5 about here]

In the relaxation process, three hard constraints are dualized into the objective function with three sets of Lagrangian multipliers firstly. To give a more clear overview of the model structure, we reorganize the variables and symbols in the objective function, and the systematic formulations are given below:

$$\left\{ \begin{array}{l} \min \sum_{s=1}^S \sum_{(i,j) \in N} \sum_{t \in T} g_{ijt}^s x_{ijt}^s - \sum_{(i,j) \in N} \left(\sum_{s=1}^S \beta_{ij}^s + \gamma_{ij} \right) \bar{x}_{ij} - \alpha S \cdot \bar{E} \\ s.t. \\ \text{constraint (10)} \\ x_{ijt}^s \in \{0, 1\}, \forall (i, j) \in N, s \in \{1, 2, \dots, S\}, t \in T \\ \bar{x}_{ij} \in [0, 1], \forall (i, j) \in N \end{array} \right. \quad (17)$$

in which g_{ijt}^s denotes the generalized link cost defined as follows.

$$g_{ijt}^s = \begin{cases} \alpha e_{ijt}^s + \beta_{ij}^s + \gamma_{ij}/S + 1, & \text{if } i = J, j = J' \text{ and } t > \widehat{T} \\ \alpha e_{ijt}^s + \beta_{ij}^s + \gamma_{ij}/S, & \text{otherwise} \end{cases} \quad (18)$$

3.2 Model decomposition

According to Fisher [10], the optimal value of the relaxed model is a lower bound of the original problem. To get the optimal objective in the relaxed model easily, we decompose the relaxed model with

respect to different parts of the objective because no coupling constraints are among them. Consequently, model (17) is finally decomposed into the following two types of sub-problems.

Sub-problem 1: $L_x(\alpha, \beta, \gamma, s)$:

The first part of model (17) can also be easily separated into a total number S shortest path problems with respect to S samples. For each space-time shortest path problem, the label setting/correction algorithm can be employed to efficiently find its optimal solutions. The subproblem over sample s (denoted by $L_x(\alpha, \beta, \gamma, s)$) is formulated as follows.

$$L_x(\alpha, \beta, \gamma, s) : \begin{cases} \min & \sum_{(i,j) \in N} \sum_{t \in T} g_{ijt}^s x_{ijt}^s \\ s.t. & \sum_{(i_t, j_t) \in N^s} x_{ijt}^s - \sum_{(j_t, i_t) \in N^s} x_{jit}^s = b_s \\ & x_{ijt}^s \in \{0, 1\}, \forall (i, j) \in N, t \in T \end{cases} \quad (19)$$

where $b_s = 1$, if $i = I, t = t_0$; $= -1$, if $i = J', t = t_0 + K\delta$; $= 0$, otherwise.

Sub-problem 2: The second sub-problem is related to the optimization with respect to decision variable \bar{x}_{ij} . Typically, this sub-problem is also separable according to individual links. Thus, the optimal solution of this problem can be easily deduced. In detail, for each link $(i, j) \in N$, it is necessary for us to calculate the following simple univariant linear programming denoted by $L_{\bar{x}}(\beta, \gamma, i, j)$.

$$L_{\bar{x}}(\beta, \gamma, i, j) : \max \left\{ \left(\sum_{s=1}^S \beta_{ij}^s + \gamma_{ij} \right) \bar{x}_{ij} : \bar{x}_{ij} \in [0, 1] \right\} \quad (20)$$

As there is only one variable in this model, the optimal solution is closely dependent on the input parameters β_{ij}^s and γ_{ij} . That is, the optimal solution \bar{x}_{ij}^* is given as below, i.e., $= 1$, if $\sum_{s=1}^S \beta_{ij}^s + \gamma_{ij} \geq 0$; $= 0$, otherwise.

The rest part of the objective function in the relaxed model is denoted by $L = \alpha S \cdot \bar{E}$. Then, for any given Lagrangian multipliers (α, β, γ) , the optimal value of the relaxed model can be easily calculated by Eq.(21), which produces an effective lower bound to the original model.

$$L(\alpha, \beta, \gamma) = \sum_{s=1}^S L_x(\alpha, \beta, \gamma, s) - \sum_{(i,j) \in N} L_{\bar{x}}(\beta, \gamma, i, j) - L \quad (21)$$

To get the tightest lower bound for the original problem, we need to solve the Lagrangian dual problem which is formulated on the basis of the relaxed model, given below.

$$L^*(\alpha, \beta, \gamma) = \max_{\alpha \geq 0, \beta \geq 0, \gamma \in \mathbb{R}} L(\alpha, \beta, \gamma) \quad (22)$$

3.3 Solution algorithms

In this paper, we use the sub-gradient algorithm to solve the Lagrangian dual problem to generate the tightest lower bound to the original problem, and the upper bound of the primal model will also be updated iteratively to reduce the gap between the upper and lower bounds. Once the minimum gap is found, the corresponding upper bound will be treated as a near-optimal objective.

Clearly, in solving the Lagrangian dual problem, we need to generate a total of S space-time paths by model (19) for each (α, β, γ) . If these space-time paths are projected into the physical network, we can

finally generate a series of physical paths, which will be used to update the upper bounds. That is, if any physical path is a feasible solution to the original problem, we then use it to update the upper bound. In the following, we give a detailed procedure of the solution algorithm (see Table 4 for the meanings of each notation), which is also displayed by a flow chart in Fig. 5.

Step 1. Initialization

Step 1.1 The iteration index in the searching process is set as d , and initialize $d=0$.

Step 1.2 The minimum upper bound of the original problem at iteration d is set as UB^d , and initialize UB^0 as a sufficiently large number. Initialize Lagrangian multipliers vector $(\alpha^0, \beta^0, \gamma^0)$ which are randomly generated from a pre-specified range.

Step 2. Lower bounds

Step 2.1 Solve the model (19) over each sample by the label-correcting algorithm. When solving the model (19) with the given Lagrangian multiplier vector $(\alpha^d, \beta^d, \gamma^d)$, we can obtain a series of S solutions X_s^d . The objective value of model (19) in iteration d is defined as $L_x^d(\alpha, \beta, \gamma, s)$, and thus $\sum_{s=1}^S L_x^d(\alpha, \beta, \gamma, s)$ can be obtained to calculate Eq. (21).

Step 2.2 Calculate the model (20) and the constant L with given Lagrangian multipliers $(\alpha^d, \beta^d, \gamma^d)$. The objective value of model (20) and the constant L in iteration d are denoted as $L_{\bar{x}}^d(\beta, \gamma)$ and L^d , separately.

Step 2.3 Obtain the objective value of model (21) in iteration d denoted by $L^d(\alpha, \beta, \gamma)$ with objective values of L^d and two subproblems, i.e., $L_x^d(\alpha, \beta, \gamma)$ and $L_{\bar{x}}^d(\beta, \gamma)$.

Step 2.4 Denote the lower bound in iteration d as LB^d which equals to the objective value $L^{*d}(\alpha, \beta, \gamma)$ of the Lagrangian dual model (22).

Step 3. Upper bounds

Step 3.1 Transform solution X_s^d over each sample into its corresponding physical path X^d . If the physical path X^d satisfies all the side constraints in original model (12), it is a feasible solution for the original problem. Otherwise, the physical path is infeasible for the original problem.

Step 3.2 The upper bound UB_s^d represents the feasible physical path's probability of late arrival in iteration d . As for the infeasible solution, UB_s^d will be set as $UB_s^d = S + 1$.

Step 3.3 Let UB^d be the minimum upper bound of the original problem and update UB^d by Eq. (23).

$$UB^d = \min\left\{ \min_{s \in \{1, 2, \dots, S\}} UB_s^d, UB^{d-1} \right\}. \quad (23)$$

Step 4. Compute the gap

Compute the gap between LB^d and UB^d by $Gap = UB^d - LB^d$. If iteration index d is greater than the predetermined maximum iteration number or the Gap is less than the predetermined value, algorithms will be terminated. Otherwise, go to step 5.

Step 5. Update the Lagrangian multipliers

The Lagrangian multiplier vector in iteration d is denoted as $(\alpha^d, \beta^d, \gamma^d)$, and the optimal solution obtained by solving model (19) and (20) in iteration d is denoted as $x_{ijt}^{s,d}$ and \bar{x}_{ij}^d , $(i, j) \in N$, $s \in \{1, 2, \dots, S\}$. In next iteration $d+1$, the Lagrangian multiplier vector for each $(i, j) \in N$, $s \in \{1, 2, \dots, S\}$ will be updated along the sub-gradient directions by Eqs. (24)-(26).

$$\alpha^{d+1} = \alpha^d + \theta^d \left(\sum_{s=1}^S \sum_{(i,j) \in N} \sum_{t \in T} e_{ijt}^s x_{ijt}^{s,d} - S \cdot \bar{E} \right) \quad (24)$$

$$\beta_{ij}^{s,d+1} = \beta_{ij}^{s,d} + \theta^d \left(\sum_{t \in T} x_{ijt}^{s,d} - \bar{x}_{ij}^d \right) \quad (25)$$

$$\gamma_{ij}^{d+1} = \gamma_{ij}^d + \theta^d \left(\frac{1}{S} \times \sum_{s=1}^S \sum_{t \in T} x_{ijt}^{s,d} - \bar{x}_{ij}^d \right) \quad (26)$$

The step size θ^d in above equations is determined by Eq. (27), which adjust the Lagrangian multipliers together with sub-gradient directions. According to Fisher M.L.[12], this speeding up method is quite mature and practical in optimization process.

$$\theta^d = \frac{\zeta^d (UB^d - L(\alpha^d, \beta^d, \gamma^d))}{f(x_{ijt}^{s,d}, \bar{x}_{ij}^d)} \quad (27)$$

In the step size equation (27), ζ^d is set as a scalar in range of $[0, 2]$, and parameter $f(x_{ijt}^{s,d}, \bar{x}_{ij}^d)$ given below is related to sub-gradient directions of the Lagrangian multiplier vector $(\alpha^d, \beta^d, \gamma^d)$.

$$f(x_{ijt}^{s,d}, \bar{x}_{ij}^d) = \left\{ \left(\sum_{s=1}^S \sum_{(i,j) \in N} \sum_{t \in T} e_{ijt}^s x_{ijt}^{s,d} - S \cdot \bar{E} \right)^2 + \sum_{s=1}^S \sum_{(i,j) \in N} \left(\sum_{t \in T} x_{ijt}^{s,d} - \bar{x}_{ij}^d \right)^2 + \sum_{(i,j) \in N} \left(\frac{1}{S} \times \sum_{s=1}^S \sum_{t \in T} x_{ijt}^{s,d} - \bar{x}_{ij}^d \right)^2 \right\}^{\frac{1}{2}}$$

Then, update iteration index $d = d + 1$, and go to step 2.

[place Fig. 5 about here]

In addition, note that in each iteration, model (19) should be solved by label correcting algorithms with the updated Lagrangian multipliers. Because we do not restrict the value of γ_{ij} , it is possible for the generalized cost g_{ijt}^s in model (19) to be negative values. In the label correcting algorithm, problems about endless cycles may happen with the negative generalized cost and the final generated time-dependent shortest path may also contain loops. Thus, the newly updated Lagrangian multipliers are suggested to be confined by the following condition based on the non-negativity of the generalized cost.

$$g_{ijt}^s = \begin{cases} \alpha e_{ijt}^s + \beta_{ij}^s + \gamma_{ij}/S + 1 \geq 0, & \text{if } i = J, j = J' \text{ and } t > \hat{T} \\ \alpha e_{ijt}^s + \beta_{ij}^s + \gamma_{ij}/S \geq 0, & \text{otherwise} \end{cases} \quad (28)$$

Through this treatment, it is expected to cancel the negative cycles in the path searching process.

4 Numerical experiments

To test the performance of the proposed approaches in this paper, this section particularly takes three networks into the consideration as the experimental environments, including an illustrative network, Sioux Falls network and West Jordan network (Salt Lake City Metropolitan Area). The algorithm encoded in the Visual Studio 2010 platform is implemented on a personal computer with Windows 7.0 platform, 2.30 GHz Central Processing Unit (CPU) and 4 Gigabyte (GB) memory. The sample-based time-variant link travel times are generated randomly based on the road distance and speed limits in these transportation networks, after which the average speeds are calculated according to the equation (1). With emission rates obtained by average speeds and emission-speed quadratic functions by Li et al. [19], we calculate the sample-based time-variant link emissions corresponding to their emission rates and link distance. In the implementations, time thresholds are selected randomly within time horizon, and emission thresholds are set by calculating link length and CO₂ emission standards referred from EPA.

4.1 Illustrative Network

In this example, we first consider a simplified three-node transportation network to test the proposed algorithm. In the implementation, the considered time horizon is set as 6 minutes which are separated by a 0.1-min interval, and then total number of considered time intervals is 60. The data needed in this small test are sample-based time-variant travel times and emissions which are randomly pre-generated.

[place Fig. 6 about here]

In this tiny acyclic transportation network, we set node 1 and node 3 as the origin node and destination node, respectively. Obviously, there exist only two paths in this OD pair, i.e., $1 \rightarrow 2 \rightarrow 3$ and $1 \rightarrow 3$. Table 6 enumerates all the total travel times and emissions of space-time paths over 10 samples.

With the given time threshold and average emission threshold, the optimal results of the eco-reliable path in this three-node network can be calculated trivially by the enumeration method (see Table 6). In this experiment, the time threshold and average emission threshold are set as 3.1 minutes and 2.6 kilograms CO₂, respectively. We first compute the shortest space-time path on different samples with the least total travel time, and then determine the feasible solution to the original problem through comparing the expected emission and its threshold. In detail, it follows from Table 6 that the paths $1 \rightarrow 2 \rightarrow 3$ and $1 \rightarrow 3$ have four and five the least time space-time paths which are later than the time threshold. At the same time, only the average emission on path $1 \rightarrow 2 \rightarrow 3$ is less than average emission threshold. Thus, the most eco-reliable physical path in this time-variant and stochastic three-node network turns out to be $1 \rightarrow 2 \rightarrow 3$.

[place Table 6 about here]

Next, we aim to use the Lagrangian relaxation approaches to solve this simple example to demonstrate the effectiveness of the proposed algorithm. In this process, we firstly find a relatively good initial Lagrangian multipliers at the beginning of the searching algorithm. In detail, we first generated a sets of Lagrangian multipliers in interval $[-5, 5]$. Then, for each Lagrangian multipliers vector in this set, we generate the lower and upper bounds with one iteration. The Lagrangian multipliers corresponding to the least gap in this set can be regarded as the initial multipliers. In addition, considering the characteristics of the proposed model, we need to generate 30 multipliers associated with unique path constraints, 3 multipliers associated with mean selection constraints and 1 multiplier for total emission constraints.

In the searching process, the Lagrangian multipliers will be updated by the sub-gradient method in each iteration, in which the lower and upper bounds can also be updated iteratively. In order to show the solution characteristics, we give Table 7 to list all the lower bounds, upper bounds and gaps (i.e., Gap) in different iterations. Clearly, with the increase of iterations, gaps between the lower and upper bounds decrease drastically. In the first iteration, the returned gap is a relatively large value (i.e., 5.199), and up to iteration 11, the gap can be reduced to almost zero, demonstrating the effectiveness of the designed algorithm. For a straightforward view, Fig. 7 gives the variation tendency curves of the lower and upper bounds in different iterations. In this figure, it is clear that the upper and lower bounds can merge with each other gradually in the first eleven iterations. Since the objective function of the original model takes integer value, the exact optimal solution is actually generated at the end of the algorithm. The most eco-reliable path turns out to be $1 \rightarrow 2 \rightarrow 3$, which just coincides with the results by enumeration methods.

[place Table 7 about here]

[place Fig. 7 about here]

4.2 Sioux Falls network

To further demonstrate the effectiveness of the proposed approach, we here consider a medium-scale transportation network as the experiment environment in Fig. 8, i.e., Sioux Falls network with 24 nodes and 76 links, which has been used in the literature for testing different path finding models, e.g., Li et al. [19], and Yang and Zhou [38]. To characterize the dynamics of link travel times, one hour time horizon is taken into consideration and discretized into a total of 120 time intervals by a 0.5-min time interval. For each OD pair with its specific time threshold and emission threshold, we should consider a total of 837 Lagrangian multipliers, including 760 Lagrangian multipliers with respect to β_{ij}^d , 76 Lagrangian multipliers with respect to γ_{ij} and one Lagrangian multiplier with respect to α . In addition, for each sample, we use the following procedure to generate the dynamic link travel time data and emission data.

Step 1: Input related data (i.e., link distance and speed limit) of the tested network;

Step 2: We compute the least link travel time with link distance and speed limit, which serves as the seeds for generating sample-based dynamic link travel times. Then, we generate the link emission rate with the speed limit, and produce the basic link emission;

Step 3: For each sample and timestamp, generate time-variant travel times and emissions through multiplying the above travel times and emissions by a random number, respectively, where the random numbers is generated in interval $[0.8, 1.5]$.

[place Fig. 8 about here]

(1) Tests with different OD pairs. Next, we first test the algorithm with the randomly generated OD pairs. In detail, we consider a total of four OD pairs as the experimental cases with the same emission standards to find the most eco-reliable path for each OD pair. As shown in Table 8, for each OD pair, we set its corresponding time threshold and emission threshold according to the driver's desirability and emission standards with respect to the path distance. Typically, in this set of experiments, all the generated lower bounds can converge to their individual upper bounds gradually with the relative small gaps (less than 0.005). In this case, each test can output the exact optimal solution in the searching process, demonstrating the effectiveness of the designed algorithm.

Likewise, Fig. 9 also shows the variant tendency curves of the returned gaps in the solution process for different OD pairs. In the updating process, the gap of each OD pair is relative large with the initial Lagrangian multipliers. With the update process of Lagrangian multipliers in the sub-gradient method, all the gaps between the lower and upper bounds decrease gradually. Although the decreasing curves of gaps over these OD pairs are distinctive, the gap curves can converge to the x-coordinate within 20 iterations. In a word, the proposed algorithm in this paper can find the exact eco-reliable paths effectively and efficiently.

[place Table 8 about here]

[place Fig. 9 about here]

(2) Tests with different emission thresholds. Next, we investigate how the emission thresholds affect the finding of optimal solutions. In detail, we shall give a series of numerical experiments with different emission thresholds based on the standard emissions, and meanwhile the time thresholds are kept invariant. To test the effectiveness of the proposed approaches in the experiments, two OD pairs are adopted randomly in Sioux Falls transportation network, namely $3 \rightarrow 18$ and $1 \rightarrow 19$.

Table 9 lists the corresponding experimental results for OD pair $3 \rightarrow 18$, in which the emission thresholds are changed from 24.0 to 26.0 kilograms CO_2 with 0.5-kilogram CO_2 increment in each case, while the time thresholds are kept as 31.0 minutes in all the tests. Likewise, we also give the experimental results for OD pair $1 \rightarrow 19$ in Table 10, where the emission thresholds are set in interval $[35.0, 37.0]$ (unit: kilograms CO_2). Clearly, in this two cases, the final gaps are all less than 0.005 despite of adopting different emission thresholds, and there are even no gaps for some tests. Thus, the quality of the optimal solutions is not much sensitive to emission thresholds in the experiments. Practically, different emission thresholds can in essence reflect various vehicle emission standards. Thus, newly updated emission standards or emission standards in different countries can still work well in this proposed model to give a high-quality route guidance. In order to reduce CO_2 emissions, governments usually mandate tighter and more aggressive emission standards. To this end, the policymakers can make the reasonable CO_2 emission standard potentially based on the sensitivity analysis with respect to emission thresholds in eco-reliable path finding model.

[place Table 9 about here]

[place Table 10 about here]

(3) Tests with different time thresholds. In the following, we are also interested in investigating the influence of time thresholds on the final gaps produced by the algorithm. For this purpose, we still use OD pairs $3 \rightarrow 18$ and $1 \rightarrow 19$ as the experimental input data. In this set of experiments, the emission thresholds are required to be invariant, while the time thresholds are changed within a range to test the sensitivity. Tables 11 and 12 are given to show the detailed computational results by adopting different parameters. Obviously, all the gaps in Tables 11 and 12 are below 0.003, even equal to zero, demonstrating the effectiveness of the proposed approaches.

On the other hand, the time thresholds can affect the eco-reliable path finding process more directly in comparison with emission thresholds. It can be seen in Tables 11 and 12 that the final lower and upper bounds are more sensitive with respect to the time thresholds, since different parameters can lead to diverse bound values. However, we note that the final quality of the solutions is also insensitive to the time thresholds because all the tests have extremely small gaps which are close to zero. Actually, the time thresholds are determined by travelers expectations, i.e., their reasonable expected arriving time. Even for the similar trips with the same OD pair, different travellers have their specific expected arriving time for various demands. The insensitive results about time thresholds imply that this eco-reliable path finding model can satisfy travelers elastic demands about arriving time to generate eco-reliable route guidance.

[place Table 11 about here]

[place Table 12 about here]

4.3 West Jordan network

To further show the performance of the proposed approaches, this section intends to implement a series of numerical experiments by using the node-link structure of West Jordan network (Salt Lake City Metropolitan Area) with 144 nodes and 354 links. In this test, we use a total of ten samples to capture the randomness of the network. Due to the short length of links in West Jordan network, the considered time horizon is set as 13 minutes which is discretized by a 0.1-min time interval, leading to 130 intervals

in the input data. The sample-based time-variant link travel times and emissions are generated by the similar procedure in section 4.2.

In this set of experiments, we randomly select five OD pairs with different time thresholds and emission thresholds to test the effectiveness of algorithms. The relevant computational results are shown in Table 13. It follows from the computational results that the gaps of different OD pairs are all close to zero, which indicates performance of the algorithm in finding the most eco-reliable path. Thus, the most eco-reliable model with the Lagrangian relaxation-based approach can provide the close-to-optimal solutions even in the large transportation network. As shown in Table 13, O_1D_1 , O_2D_2 , O_3D_3 , O_4D_4 , O_5D_5 represent five tested OD pairs, i.e., $5436 \rightarrow 11129$, $11125 \rightarrow 5592$, $5113 \rightarrow 11507$, $1296 \rightarrow 11489$, $5018 \rightarrow 10857$, respectively. For clarity, we also use different colors to identify the OD pairs based optimal paths obtained by our proposed approaches in Fig.10.

[place Fig. 10 about here]

[place Table 13 about here]

5 Conclusions and future research

To formulate the reliability and ecology of the path finding problem in time-variant and stochastic transportation networks, this paper proposed a new definition of the most eco-reliable path which can arrive at the destination on time and meet emission standards potentially imposed by government regulators. To characterize the dynamics and randomness in the network, we discretized the considered time horizon to capture the dynamics of the link travel times and emissions, and we used different samples to describe the inherent randomness. With the given dynamic and stochastic travel times and emissions, we formulated an integer programming model for finding the most eco-reliable path, in which the objective function aims to measure the on-time arrival probability and the emission threshold is given to restrict the emissions. To effectively solve the proposed model, a Lagrangian relaxation based algorithmic framework was proposed to find the near-optimal solutions. In detail, some hard constraints were first dualized into the objective functions through introducing a series of Lagrangian parameters. Then the relaxed model was decomposed into different simple sub-problems, which can be easily handled by the existing algorithm. A sub-gradient algorithm was adopted to iteratively reduce the gaps between the lower and upper bounds. The results of these numerical experiments, above all the experiments in real transportation networks (i.e., the Sioux Falls network and the West Jordan network (Salt Lake City Metropolitan Area)), demonstrate that the proposed approach can generate high-quality solutions with small gaps, which can typically provide travelers with eco-reliable route guidance.

In this paper, we discussed the CO_2 emission reductions in individual trips and proposed a new definition of the most eco-reliable path which can arrive at the destination on time and meet emission standards. Practically, we can use the real-world detected data in the decision-making problem, i.e., the eco-reliable path finding model, and obtain high-quality solutions. After analyzing results in numerical experiments, it shows that this eco-reliable path finding model can satisfy the demands of both travelers and government regulators. According to the eco-reliable path finding model, effective emission policies about in-use vehicles can be expectedly made and implemented in intelligent transportation systems. Therefore, this model is suitable to support the further development in real applications.

Further research of the most eco-reliable path finding can be focused on the following three aspects. (1) This study only investigates the methods for generating the a priori path with the guaranteed reliability

and restricted emissions. In more complex cases, how to embed the adaptive strategy into the path finding process so as to produce the adaptively generated eco-reliable path can be a new topic in our further study. (2) For many large-scale problems, we still need to explore more efficient searching algorithms as the sub-gradient algorithm is not stable sufficiently in some cases. Then, designing hybrid algorithms with other searching strategies (e.g., branch and bound algorithm, heuristics, etc.) is also an interesting research topic. (3) To find the eco-reliable path, we just consider CO₂ emissions in this paper. Energy consumption should also be taken into consideration in the future research.

Acknowledgement

The research of this paper was supported by the National Natural Science Foundation of China (Nos: 71271020, 71422002, 71621001).

References

- [1] Akcelik R. and Besley M. (2007) Operating cost, fuel consumption and emission models in aaSIDRA and aaMOTION. In: 25th Conference of Australian Institutes of Transport Research (CAITR 2003) University of South Australia, Adelaide, Australia.
- [2] Aziz H.M.A. and Ukkusuri S.V. (2014) Exploring the trade-off between greenhouse gas emissions and travel time in daily travel decisions: route and departure time choices. *Transportation Research Part D: Transport and Environment*, 32, 334-353.
- [3] Bertsekas D. P. (1992) A simple and fast label correcting algorithm for shortest paths. *Networks*, 23(7), 703-709.
- [4] Barth M., Younglove T. and Scora, G. (2005) Development of a heavy-duty diesel modal emissions and fuel consumption model. Technical report. UCB-ITS-PRR-2005-1, California Path Program, Institute of Transportation Studies, University of California at Berkeley.
- [5] Bektas T. and Laporte G. (2011) The pollution-routing problem. *Transportation Research Part B: Methodological*, 45(8), 1232-1250.
- [6] Erdogan S. and Miller-Hooks E. (2012) A green vehicle routing problem. *Transportation Research Part E: Logistics and Transportation Review*, 109(1), 100-114.
- [7] Edenhofer O., Pichs-Madruga R., Sokona Y., Kadner S., Minx J.C., Brunner S., et al. (2014) Technical summary. In: Edenhofer O., Pichs-Madruga R., Sokona Y., Farahani E., Kadner S., Seyboth K., et al., editors. *Clim. Chang. 2014 Mitig. Clim. Chang. Contrib. Work. Gr. III to Fifth Assess. Rep. Intergov. Panel Clim. Chang.* Cambridge, United Kingdom and New York, NY, USA: Cambridge University Press.
- [8] EPA U. (2015) User guide for MOVES2014a. Technical report, United States Environmental Protection Agency.
- [9] Ehmke J.F., Campbell A.M. and Thomas B.W. (2015) Vehicle routing to minimize time-dependent emissions in urban areas. *European Journal of Operational Research*, 251(2), 478-494.

- [10] Fisher M.L. (1985) An Applications Oriented Guide to Lagrangian Relaxation. *Interfaces*, 15(2), 10-21.
- [11] Fan Y.Y., Kalaba R.E. and Moore J.E. (2005) Arriving on time. *Journal of Optimization Theory and Applications*, 127(3), 497-513.
- [12] Fisher M.L. (2004) The Lagrangian Relaxation Method for Solving Integer Programming Problems. *Management Science*, 50(12 Supplement), 1861-1871.
- [13] Geoffrion A. (2009) Lagrangian Relaxation for Integer Programming. 50 Years of Integer Programming 1958-2008, 243-281.
- [14] Hu X., Chang S., Li J. and Qin Y. (2010) Energy for sustainable road transportation in China: challenges, initiatives and policy implications. *Energy*, 35(11), 4289-4301.
- [15] Heinrichs H., Jochem P. and Fichtner W. (2014) Including road transport in the EU ETS (European Emissions Trading System): A model-based analysis of the German electricity and transport sector. *Energy*, 69(5), 708-720.
- [16] Hao H., Liu Z., Zhao F., Li W. and Hang W. (2015) Scenario analysis of energy consumption and greenhouse gas emissions from China's passenger vehicles. *Energy*, 91, 151-159.
- [17] Huang Y., Yang L., Tang T., Cao F. and Gao Z. (2016) Saving Energy and Improving Service Quality: Bicriteria Train Scheduling in Urban Rail Transit Systems. *IEEE Transactions on Intelligent Transportation Systems*, 17, 1-16.
- [18] Knörr W. (2008) EcoTransIT: ecological transport information tool-environmental methodology and data. Tech. rep., Institut für Energie (ifeu) und Umweltforschung Heidelberg GmH (accessed 11.02.11).
- [19] Li Q., Nie Y.M., Vallamsundar S., Lin J. and Homem-de-Mello T. (2014) Finding efficient and environmentally friendly paths for risk-averse freight carriers. *Networks and Spatial Economics*, 1-21.
- [20] Li W., Dai Y., Ma L., Hao H., Lu H., Albinson R. and Li Z. (2015) Oil-saving pathways until 2030 for road freight transportation in China based on a cost-optimization model. *Energy*, 86, 369-384.
- [21] Liu J. and Zhou X. (2016) Capacitated transit service network design with boundedly rational agents. *Transportation Research Part B: Methodological*, 93, 225-250.
- [22] Lu C.C., Liu J., Qu Y., Peeta S., Roupail N.M. and Zhou X. (2016) Eco-system optimal time-dependent flow assignment in a congested network. *Transportation Research Part B: Methodological*, 94, 217-239.
- [23] Mahmoudi M. and Zhou X. (2016) Finding optimal solutions for vehicle routing problem with pickup and delivery services with time windows: a dynamic programming approach based on state-space-time network representations. *Transportation Research Part B: Methodological*, 89, 19-42.
- [24] Miller-Hooks E. (2001) Adaptive least-expected time paths in stochastic, time-varying transportation and data networks. *Networks*, 37(1), 35-52.

- [25] Nagurney A. (2000) Congested urban transportation networks and emission paradoxes. *Transportation Research D*, 5(2), 145-151.
- [26] Nielsen L.R. (2003) Route choice in stochastic time-dependent networks. Ph.D. Dissertation. University of Aarhus, USA.
- [27] Nie Y.M. and Wu X. (2009) Shortest path problem considering on-time arrival probability. *Transportation Research Part B: Methodological*, 43(6), 597-613.
- [28] Nie Y.M. and Li Q. (2013) An eco-routing model considering microscopic vehicle operating conditions. *Transportation Research Part B: Methodological*, 55, 154-170.
- [29] Palmer A. (2007) The Development of an integrated routing and carbon dioxide emissions model for good vehicles. Ph.D. Dissertation. Cranfield University, UK.
- [30] Rilett L. and Benedek C. (1994) Traffic assignment under environmental and equity objectives. *Transportation Research Record*, 1443, 29-37.
- [31] Simpson A.G. (2005) Parametric modeling of energy consumption in road vehicles. Ph.D. Dissertation. The University of Queensland, Australia.
- [32] Samaranayake S., Blandin S. and Bayen A. (2011) A tractable class of algorithms for reliable routing in stochastic networks. *Procedia-Social and Behavioral Sciences*, 17, 341-363.
- [33] Tzeng G. and Chen C. (1993) Multiobjective decision making for traffic assignment. *IEEE Transportation Engineering Management*, 2, 180-187.
- [34] Walmsley M.R.W., Walmsley T.G., Atkins M.J. et al. (2015) Carbon Emissions Pinch Analysis for emissions reductions in the New Zealand transport sector through to 2050. *Energy*, 92, 569-576.
- [35] Wang L., Gao Z. and Yang L. (2016) A priori least expected time paths in fuzzy, time-variant transportation networks. *Engineering Optimization*, 48(2), 272-298.
- [36] Xu B. and Lin B. (2015) Carbon dioxide emissions reduction in China's transport sector: A dynamic VAR (vector autoregression) approach. *Energy*, 83, 486-495.
- [37] Yin Y. and Lawphongpanich S. (2006) Internalizing emission externality on road networks. *Transportation Research Part D: Transport and Environment*, 11(4), 292-301.
- [38] Yang L. and Zhou X. (2014) Constraint reformulation and a Lagrangian relaxation-based solution algorithm for a least expected time path problem. *Transportation Research Part B: Methodological*, 59, 22-44.
- [39] Yang L., Zhou X. and Gao Z. (2014) Credibility-based rescheduling model in a double-track railway network: a fuzzy reliable optimization approach. *Omega*, 48, 75-93.
- [40] Yang L., Li S., Gao Y. and Gao Z. (2015) A coordinated routing model with optimized velocity for train scheduling on a single-track railway line. *International Journal of Intelligent Systems*, 30, 3-22.
- [41] Yang L., Zhang Y., Li S. and Gao Y. (2016) A two-stage stochastic optimization model for the transfer activity choice in metro networks. *Transportation Research Part B: Methodological*, 83, 271-297.

- [42] Yin J., Tang T., Yang L., Gao Z. and Ran B. (2016) Energy-efficient metro train rescheduling with uncertain time-variant passenger demands: An approximate dynamic programming approach. *Transportation Research Part B: Methodological*, 91, 178-210.
- [43] Yang L. and Zhou X. (2017) Optimizing on-time arrival probability and percentile travel time for elementary path finding in time-dependent transportation networks: Linear mixed integer programming reformulations. *Transportation Research Part B: Methodological*, 96, 68-91.
- [44] Zhou X., Tanvir S., Lei H., Taylor J., Liu B., Roupaild N.M. and Frey H.C. (2015) Integrating a simplified emission estimation model and mesoscopic dynamic traffic simulator to efficiently evaluate emission impacts of traffic management strategies. *Transportation Research Part D: Transport and Environment*, 37, 123-136.
- [45] Zeng W., Miwa T. and Morikawa T. (2016) Prediction of vehicle CO₂ emission and its application to eco-routing navigation. *Transportation Research Part C: Emerging Technologies*, 68, 194-214.

The List of Tables:

Table 1 The main features of different studies

Table 2 Parameters and decisions variables used in formulation

Table 3 Total travel times and emissions over different samples

Table 4 Average emissions for passenger cars from EPA

Table 5 Symbols used in the Lagrangian relaxation algorithm

Table 6 Total travel time and total emission of two paths over 10 samples

Table 7 Computational Results by the Lagrangian relaxation approach

Table 8 Results for the Sioux Falls transportation networks with different OD pairs

Table 9 Results with different emission thresholds for OD pair 3 → 18

Table 10 Results with different emission thresholds for OD pair 1 → 19

Table 11 Results with different time thresholds for OD pair 3 → 18

Table 12 Results with different time thresholds for OD pair 1 → 19

Table 13 Results for the Salk Lake City transportation network with different OD pairs

Table 1: The main features of different studies

Features	Bektas and Laporte [5]	Nie and Wu [27]	Li et al. [19]	This paper
Random and dynamic characteristics	No	Random link travel times	Random link travel times and emissions	Random and dynamic link travel times and emissions
Consideration of Reliability	No	Yes	Yes	Yes
Emissions	Cost of emissions	No	Monetary cost of emissions	Expected emission constraint
Objective function	Total cost of fuel consumption, emissions and paid to drivers	On-time arrival probability	Weighted combination of travel time, fuel and emissions	Late arrival probability
Solution method	CPLEX	Label correcting algorithm	CPLEX	Label-correcting algorithm, sub-gradient algorithm

Table 2: Parameters and decisions variables used in formulation

Notations	Definition
M	= Set of physical nodes
N	= Set of physical links
i, j	= Indexes of physical nodes, $i, j \in M$
(i, j)	= Index of directed physical link between adjacent nodes i and j , $(i, j) \in N$
T	= The considered time period, $T = \{t_0, t_0 + \delta, t_0 + 2\delta, \dots, t_0 + K\delta\}$
\hat{T}	= Time threshold to indicate on-time arrival
s	= Index of samples, $s \in \{1, 2, \dots, S\}$
S	= Total number of samples
P_s	= Probability of sample s , $s \in \{1, 2, \dots, S\}$
a_{ijt}^s	= Travel time on link (i, j) at entering time t on sample s
e_{ijt}^s	= Travel CO ₂ emission on link (i, j) at entering time t on sample s
x_{ijt}^s	= 1 if traffic link (i, j) is used at entering time t on sample s ; = 0 otherwise
$x_{JJ't}^s$	= 1 if dummy traffic link (J, J') is used at entering time t on sample s ; = 0 otherwise
Γ_t	= Probability of late arrival
E_{total}	= Expected vehicle emissions on the selected path
\bar{E}	= Expected emission threshold

Table 3: Total travel times and emissions over different samples

Sample	Departure time	Total travel time	Arrival time	Time threshold	Total emission
S_1	0	2	2	5	6
S_2	1	3	4	5	7
S_3	1	5	6	5	7
S_4	2	5	7	5	8
AOT Probability			50%		
Average emission					7

Table 4: Average emissions for passenger cars from EPA

Pollutant	Emission Rates (per mile driven)	Annual Emission
Volatile organic compounds (VOC)	1.034 grams (g)	27.33 pound (lb)
Total hydrocarbons (THC)	1.077 g	28.47 lb
Carbon monoxide (CO)	9.400 g	248.46 lb
Nitrogen oxides (NO _X)	0.693 g	18.32 lb
Particulate matter under 10 microns Diameter (PM ₁₀)	0.0044 g	0.12 lb
Particulate matter under 2.5 microns Diameter (PM _{2.5})	0.0041 g	0.11 lb
Carbon dioxide (CO ₂)	368.4 g	9737.44 lb

Table 5: Symbols used in the Lagrangian relaxation algorithm

Symbols	Definition
α	= Lagrangian multipliers corresponding to constraint (3)
β_{ij}^s	= Lagrangian multipliers corresponding to constraint (16)
γ_{ij}	= Lagrangian multipliers corresponding to constraint (15)
d	= Iteration index
$(\alpha^d, \beta^d, \gamma^d)$	= Vectors of Lagrangian multipliers in iteration d
$L_x^d(\alpha, \beta, \gamma, s)$	= The objective value of subproblem 1 in iteration d
$L_{\bar{x}}^d(\beta, \gamma, i, j)$	= The objective value of subproblem 2 in iteration d
L^d	= The value of L in iteration d
$L^d(\alpha, \beta, \gamma)$	= The objective value of the relaxed model in iteration d
$L^{*d}(\alpha, \beta, \gamma)$	= The objective value of the Lagrangian dual problem in iteration d
UB_s^d	= Upper bound in iteration d on sample s
UB^d	= The minimum upper bound of the original problem in iteration d
LB^d	= Lower bound in iteration d
θ^d	= Step size in iteration d
X_s^d	= Vectors of the lower bound solution in iteration d on sample s
X^d	= Vector of physical path in iteration d

Table 6: Total travel time and total emission of two paths over 10 samples

$1 \rightarrow 2 \rightarrow 3$	s=1	s=2	s=3	s=4	s=5	s=6	s=7	s=8	s=9	s=10
Total travel time	3.3	2.8	3.1	2.8	3.5	3.2	3.0	3.9	2.5	2.9
Total emission	2.7	2.3	2.6	2.3	2.9	2.6	2.5	3.3	2.1	2.5
Average emission	2.58									
$1 \rightarrow 3$	s=1	s=2	s=3	s=4	s=5	s=6	s=7	s=8	s=9	s=10
Total travel time	3.3	3.0	3.2	4.1	2.7	3.3	2.8	2.9	2.8	3.4
Total emission	2.8	2.5	2.6	3.5	2.2	2.8	2.3	2.4	2.3	2.8
Average emission	2.62									

Table 7: Computational Results by the Lagrangian relaxation approach

Iteration	Lower Bound	Upper Bound	Gap (Gap= Upper Bound - Lower Bound)
1	-1.199	4	5.199
2	0.886	4	3.114
3	0.886	4	3.114
4	1.141	4	2.859
5	1.218	4	2.782
6	1.372	4	2.628
7	2.723	4	1.277
8	3.090	4	0.910
9	3.109	4	0.891
10	3.470	4	0.530
11	3.998	4	0.002
Optimal Route:		1 → 2 → 3	

Table 8: Results for the Sioux Falls transportation networks with different OD pairs

Origin	Destination	Time Threshold (minutes)	Emission Threshold (kilograms CO ₂)	Lower Bound	Upper Bound	Gap (Gap= Upper Bound - Lower Bound)	Optimal Path
1	19	41	36	1.000	1	0.000	1 → 2 → 6 → 8 → 16 → 17 → 19
2	13	32	24	1.996	2	0.004	2 → 1 → 3 → 12 → 13
3	18	31	25	1.997	2	0.003	3 → 4 → 5 → 6 → 8 → 7 → 18
3	20	35	27	2.997	3	0.003	3 → 12 → 13 → 24 → 21 → 20

Table 9: Results with different emission thresholds for OD pair 3 → 18

Time Threshold (minutes)	Emission Threshold (kilograms CO ₂)	Lower Bound	Upper Bound	Gap (Gap= Upper Bound - Lower Bound)
31.0	24.0	1.997	2	0.003
31.0	24.5	1.997	2	0.003
31.0	25.0	1.998	2	0.002
31.0	25.5	1.997	2	0.003
31.0	26.0	1.997	2	0.003

Table 10: Results with different emission thresholds for OD pair 1 \rightarrow 19

Time Threshold (minutes)	Emission Threshold (kilograms CO ₂)	Lower Bound	Upper Bound	Gap (Gap= Upper Bound - Lower Bound)
41.0	35.0	1.000	1	0.000
41.0	35.5	1.000	1	0.000
41.0	36.0	1.000	1	0.000
41.0	36.5	1.000	1	0.000
41.0	37.0	1.000	1	0.000

Table 11: Results with different time thresholds for OD pair 3 \rightarrow 18

Time Threshold (minutes)	Emission Threshold (kilograms CO ₂)	Lower Bound	Upper Bound	Gap (Gap= Upper Bound - Lower Bound)
30.0	25.0	2.999	3	0.001
30.5	25.0	2.999	3	0.001
31.0	25.0	1.998	2	0.002
31.5	25.0	1.997	2	0.003
32.0	25.0	0.997	1	0.003

Table 12: Results with different time thresholds for OD pair 1 \rightarrow 19

Time Threshold (minutes)	Emission Threshold (kilograms CO ₂)	Lower Bound	Upper Bound	Gap (Gap= Upper Bound - Lower Bound)
40.0	36.0	2.999	3	0.001
40.5	36.0	2.999	3	0.001
41.0	36.0	1.000	1	0.000
41.5	36.0	1.000	1	0.000
42.0	36.0	-0.001	0	0.001

Table 13: Results for the Salk Lake City transportation network with different OD pairs

Origin	Destination	Time Threshold (minutes)	Emission Threshold (kilograms CO ₂)	Lower Bound	Upper Bound	Gap Gap= Upper Bound - Lower Bound	Optimal Route
5436 (O ₁)	11129 (D ₁)	3.9	3.5	2.000	2	0.000	5436 → 11125 → 5440 → 11127 → 11126 → 5441 → 5861 → 10872 → 5030 → 4958 → 1299 → 11129
11125 (O ₂)	5592 (D ₂)	5.0	4.5	3.000	3	0.000	11125 → 1289 → 11124 → 5022 → 11147 → 5820 → 5103 → 11161 → 5114 → 5592
5113 (O ₃)	11507 (D ₃)	6.7	6.0	2.999	3	0.001	5113 → 11160 → 5112 → 11172 → 1353 → 11173 → 5219 → 1355 → 11183 → 5215 → 5588 → 1357 → 5174 → 5868 → 5216 → 11507
1296 (O ₄)	11489 (D ₄)	4.7	4.2	2.000	2	0.000	1296 → 5240 → 5009 → 5027 → 11150 → 5109 → 4804 → 5106 → 5117 → 1358 → 3002 → 3001 → 8172 → 11489
5018(O ₅)	10857 (D ₅)	7.8	7.0	-0.001	0	0.001	5018 → 1289 → 11124 → 5022 → 11147 → 5820 → 5103 → 11161 → 5114 → 11173 → 5219 → 1355 → 11183 → 5215 → 6255 → 10857

The List of Figures:

- Fig.1. An illustration of space-time network and on-time arrival
Fig.2. An illustration of evaluating a path with eco-reliable index
Fig.3. Flow chart for emission estimation
Fig.4. An illustration for calculating on-time arrival probability
Fig.5. Flow chart of the solution methodology
Fig.6. Simplified three-node network
Fig.7. Variation tendency of upper and lower bounds in the searching process
Fig.8. Sioux Falls network
Fig.9. Variation tendency of gaps in Sioux Falls network
Fig.10. West Jordan network (Salt Lake City Metropolitan Area)

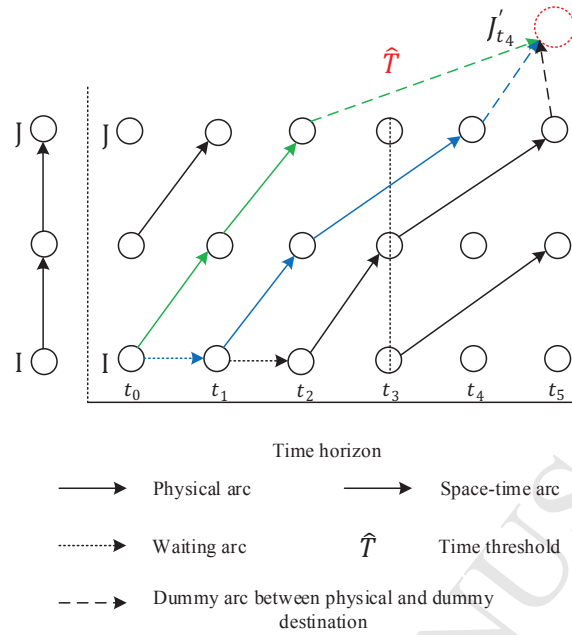


Fig.1. An illustration of space-time network and on-time arrival

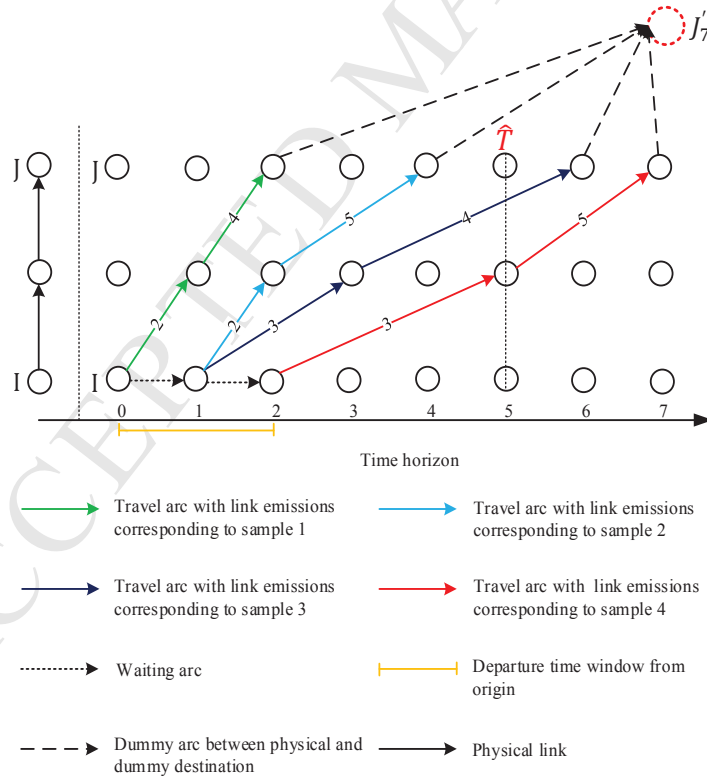


Fig.2. An illustration of evaluating a path with eco-reliable index

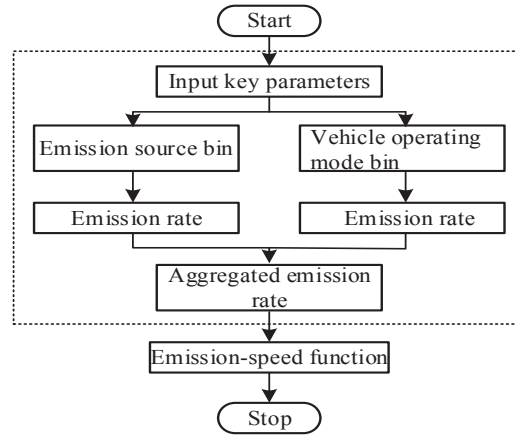


Fig.3. Flow chart for emission estimation

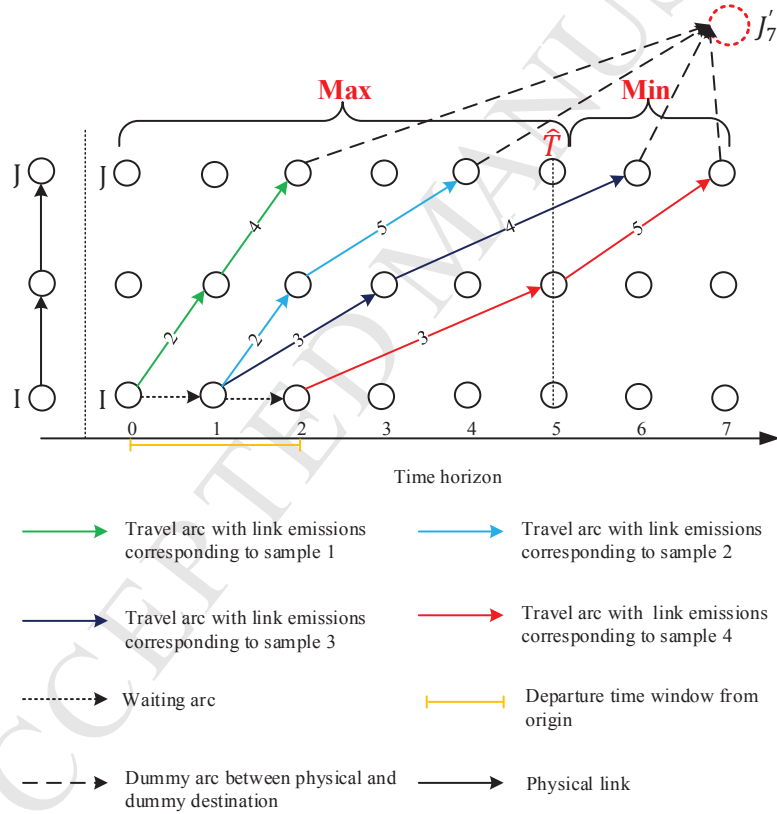


Fig.4. An illustration for calculating on-time arrival probability

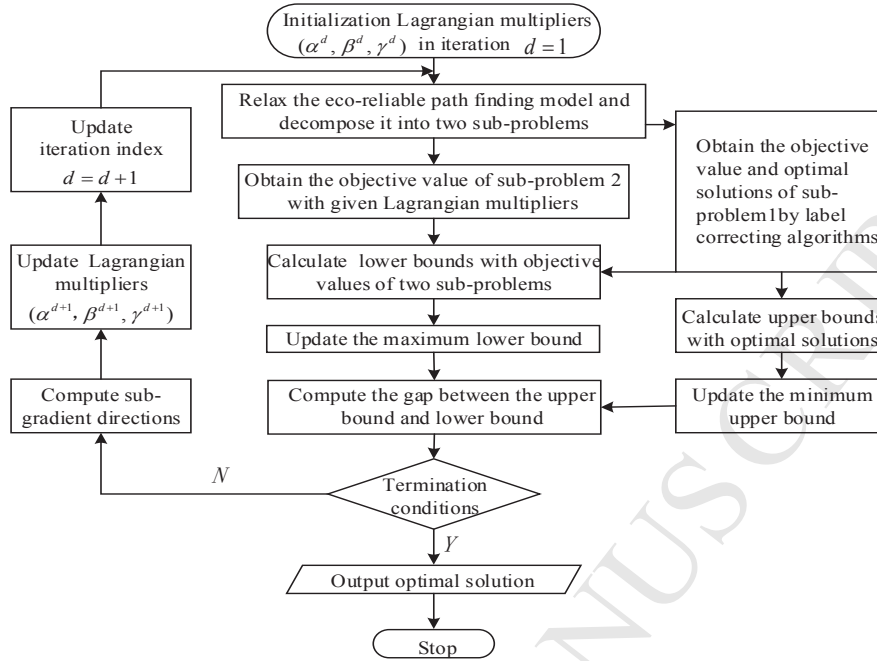


Fig.5. Flow chart of the solution methodology

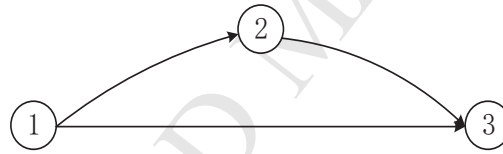


Fig.6. Simplified three-node network

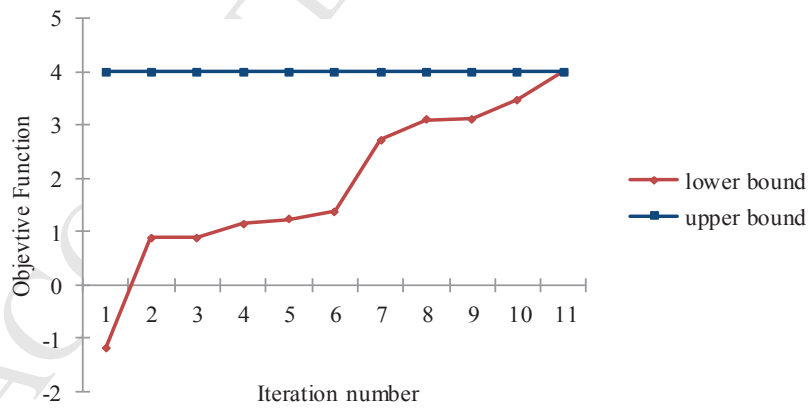


Fig.7. Variation tendency of upper and lower bounds in the searching process

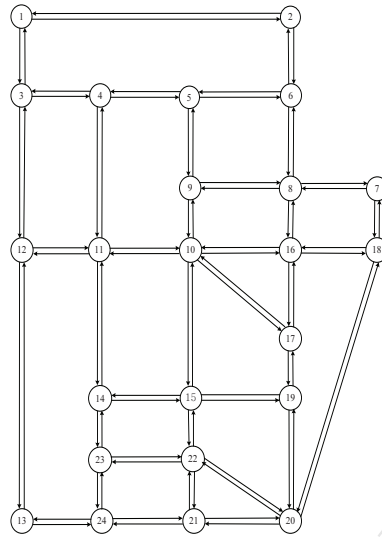


Fig.8. Sioux Falls network

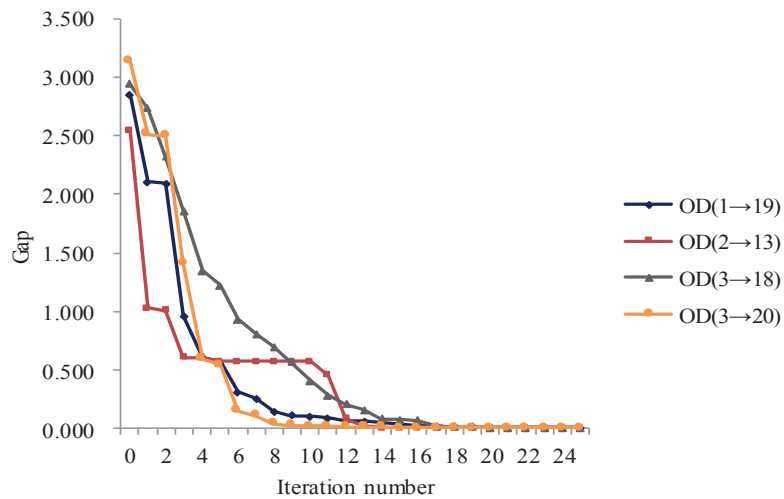


Fig.9. Variation tendency of gaps in Sioux Falls network

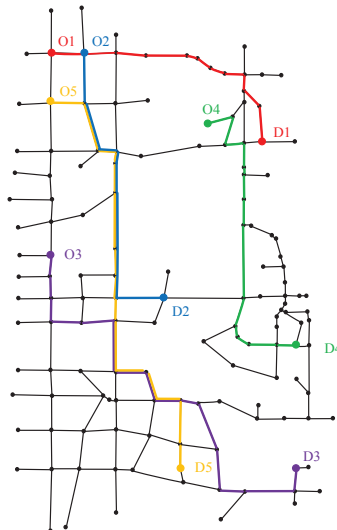


Fig.10. West Jordan network (Salt Lake City Metropolitan Area)

Highlights

- (1) The most eco-reliable path is defined in time-variant and stochastic networks.
- (2) The model is developed with on-time arrival probability and emission constraints.
- (3) The sub-gradient and label correcting algorithm are integrated to solve the model.
- (4) Numerical experiments demonstrate the effectiveness of developed approaches.

ACCEPTED MANUSCRIPT